Title	eIF5 stimulates the CUG initiation of RAN translation of poly-GA dipeptide repeat protein (DPR) in C9orf72 FTLD/ALS
Author(s)	Gotoh, Shiho; Mori, Kohji; Fujino, Yuzo et al.
Citation	Journal of Biological Chemistry. 2024, 300(3), p. 105703
Version Type	VoR
URL	https://hdl.handle.net/11094/95671
rights	This article is licensed under a Creative Commons Attribution-NonCommercial-NoDerivatives 4.0 International License.
Note	

eIF5 stimulates the CUG initiation of RAN translation of poly-GA dipeptide repeat protein (DPR) in *C9orf72* FTLD/ALS

Shiho Gotoh[1], **Kohji Mori**[1,*], **Yuzo Fujino**[2,3], **Yuya Kawabe**[1], **Tomoko Yamashita**[1], **Tsubasa Omi**[1], **Kenichi Nagata**[4], **Shinji Tagami**[1], **Yoshitaka Nagai**[2], and **Manabu Ikeda**[1]

From the [1]Department of Psychiatry, Osaka University Graduate School of Medicine, Suita, Japan; [2]Department of Neurology, Kindai University Faculty of Medicine, Osaka-Sayama, Japan; [3]Department of Neurology, Kyoto Prefectural University of Medicine, Kyoto, Japan; [4]Department of Precision Medicine for Dementia, Osaka University Graduate School of Medicine, Suita, Japan

Reviewed by members of the JBC Editorial Board. Edited by Karin Musier-Forsyth

Tandem GGGGCC repeat expansion in *C9orf72* is a genetic cause of frontotemporal lobar degeneration (FTLD) and amyotrophic lateral sclerosis (ALS). Transcribed repeats are translated into dipeptide repeat proteins *via* repeat-associated non-AUG (RAN) translation. However, the regulatory mechanism of RAN translation remains unclear. Here, we reveal a GTPase-activating protein, eukaryotic initiation factor 5 (eIF5), which allosterically facilitates the conversion of eIF2-bound GTP into GDP upon start codon recognition, as a novel modifier of *C9orf72* RAN translation. Compared to global translation, eIF5, but not its inactive mutants, preferentially stimulates poly-GA RAN translation. RAN translation is increased during integrated stress response, but the stimulatory effect of eIF5 on poly-GA RAN translation was additive to the increase of RAN translation during integrated stress response, with no further increase in phosphorylated eIF2α. Moreover, an alteration of the CUG near cognate codon to CCG or AUG in the poly-GA reading frame abolished the stimulatory effects, indicating that eIF5 primarily acts through the CUG-dependent initiation. Lastly, in a *Drosophila* model of *C9orf72* FTLD/ALS that expresses GGGGCC repeats in the eye, knockdown of endogenous eIF5 by two independent RNAi strains significantly reduced poly-GA expressions, confirming *in vivo* effect of eIF5 on poly-GA RAN translation. Together, eIF5 stimulates the CUG initiation of poly-GA RAN translation in cellular and *Drosophila* disease models of *C9orf72* FTLD/ALS.

Frontotemporal lobar degeneration (FTLD) is a neurodegenerative disease characterized by behavioral disturbances, aphasia, and dementia, with localized atrophy of the frontal and temporal lobes. Amyotrophic lateral sclerosis (ALS) is a neurodegenerative disease characterized by motor neuron degeneration and muscle weakness. These diseases present with different clinical symptoms but share common pathological mechanisms. An unusually expanded GGGGCC (G_4C_2) repeat in intron 1 of *C9orf72* gene was discovered in 2011 to be the most frequent cause of FTLD/ALS (1–3). Nonpathogenic repeat lengths have been proposed to be 2 to 30 (G_4C_2) repeats, whereas *C9orf72* FTLD/ALS (*C9*-FTLD/ALS) patients typically have hundreds to thousands of repeats. The G_4C_2 repeat is transcribed from sense and antisense strands. Subsequently, the repeat transcripts are translated into poly-GA (glycine-alanine), poly-GP (glycine-proline), and poly-GR (glycine-arginine) from sense transcript and poly-proline-alanine, poly-GP, and poly-proline-arginine from antisense transcript through repeat associated non-AUG (RAN) translation (4–9). These proteins are named dipeptide repeat proteins (DPR) based on their dipeptide motifs (5). DPR forms cytoplasmic and intranuclear inclusions in the brain of *C9*-FTLD/ALS patients. Multiple *in vitro* and *in vivo* models including yeast (10), fly (11, 12), cultured cells (13–15), and mice (16, 17) have revealed extensive DPR toxicity, although whether the accumulation of specific DPR correlates with neurodegeneration in *C9*-FTLD/ALS patients has been controversial (18–23). The other disease mechanisms including sequestration of RNA binding proteins into repeat RNA foci and/or loss of lysosome/autophagy function through reduction of C9orf72 protein may aggravate neurodegeneration in *C9*-FTLD/ALS models (24–29); current evidence supports the notion that RAN translation inhibition and thus suppression of DPR expressions would have therapeutic potential. To achieve this goal, it is essential to elucidate the precise mechanism underlying RAN translation.

As for the mechanism of RAN translation, several research groups have described cellular stress and neural excitation enhance RAN translation through eIF2α phosphorylation (30–32). Moreover, metformin, an antidiabetic, inhibits protein kinase R that targets eIF2α and thus RAN translation (33). Mechanistically, the internal ribosome entry site-related protein RPS25, RNA helicases DDX3X and DHX36, and the RNA-binding protein FUS have been reported to regulate the RAN

translation of *C9orf72* repeat (34–37). Several eukaryotic translation initiation factors (eIFs) are implicated in *C9orf72* RAN translation. Reduction in eIF4B and eIF4H, accessory proteins of the eIF4A helicase, reduces poly-GR-GFP from G_4C_2 transcripts in *Drosophila* (38). Similarly, the reduction in eIF2D, but not eIF2A, was reported to reduce the expression of poly-GA and poly-GP in a *C. elegans* model and in human-derived cell lines (39), but this was not reproduced by eIF2D knockdown in HEK293 cells (40).

The present study investigated whether eukaryotic initiation factor eIF5 (41) regulates RAN translation. Biochemical studies since 1980s have established the role of eIF5 on start site selection in general translation as a GTPase-activating protein (GAP) (42–46). In translation initiation, 43S preinitiation complex (PIC) scans through the 5′UTR region of RNA typically until it recognizes AUG initiation codon with preferred Kozak consensus sequence (47, 48), although PIC can also recognize AUG in a nonpreferred context or a near cognate codon in a preferred context with lower recognition efficiency. Subsequently, eIF5 binds to the eIF2 subunit of the 43S PIC, and this binding allosterically stimulates the hydrolysis of eIF2-bound guanosine triphosphate (GTP) to guanosine diphosphate (GDP) (49). Upon GTP hydrolysis, eIF2 loses its affinity for the initiator, Met-tRNA, leaving the PIC. The remaining part of the PIC and the newly recruited 60S ribosome subunit together form a mature 80S ribosome, and this 80S ribosome starts the synthesis of nascent polypeptides. Interestingly, increasing the level of eIF5 has been reported to reduce the stringency of start codon recognition and suppress leaky scanning, in which ribosomes skip initiation at the AUG with a suboptimal Kozak consensus sequence (50, 51).

Although an AUG in an optimal Kozak sequence is the most favorable initiation site for eukaryotic translation, RAN translation is delineated by non-AUG initiation. Especially, recent reports described that poly-GA RAN translation initiates at CUG codon in the 5′ leader sequence of G_4C_2 repeat (29, 30, 52–54).

In this study, we reveal that eIF5 preferentially stimulates CUG-dependent poly-GA RAN translation over global translation in disease models of *C9*-FTLD/ALS. Mechanistically, this effect was mediated by the GAP activity of eIF5. Moreover, substitution of CUG near cognate to <u>A</u>UG abolished the stimulatory effect of eIF5 on poly-GA RAN translation. Consistent with these findings, we also observed the stimulatory effect of eIF5 on poly-GA RAN translation in an *in vivo Drosophila* model of *C9*-FTLD/ALS. Thus, we propose that eIF5 stimulates initiation at CUG near the cognate codon during *C9orf72* poly-GA RAN translation.

Results

eIF5 positively regulates poly-GA expression through RAN translation

To monitor RAN translation in a cellular model of *C9*-FTLD/ALS, we utilized $(G_4C_2)_{80}$ repeat expression plasmids (5, 28, 55). The plasmids express transcripts containing 113 bp endogenous 5′flanking leader sequence adjacent to *C9orf72*

G_4C_2 repeats followed by pathogenic 80 repeats of tandem G_4C_2 sequence. The 5′flanking region contains a near cognate CUG codon where poly-GA translation initiates (29, 53). Additionally, the C-terminal FLAG tag was artificially fused to the poly-GA reading frame that could be initiated by CUG codon (Fig. 1*A*). Using this system, we tested the effect of eIF5 knockdown on poly-GA RAN translation in repeat-expressing HeLa cells. Knockdown of eIF5 using two different siRNAs similarly decreased cellular eIF5 expression (Fig. 1, *B* and *C*) and poly-GA expression levels (Fig. 1, *B* and *D*). These results suggest that a reduction in eIF5 suppresses poly-GA RAN translation in our cellular model of *C9*-FTLD/ALS. Next, we examined whether eIF5 expression stimulated poly-GA RAN translation. To do so, an N-terminally V5-tagged eIF5 expression plasmid, lacking the upstream open reading frame of eIF5 to avoid its own autoregulation (50), was constructed and coexpressed with the $(G_4C_2)_{80}$ repeat plasmid in HeLa cells (Fig. 1*A*). The expression levels of exogenous eIF5 were verified using anti-eIF5 and anti-V5 antibodies (Fig. 1*E*). This approach revealed that eIF5 increased poly-GA expression in the $(G_4C_2)_{80}$ repeat (Fig. 1, *E* and *F*). RT-qPCR analysis confirmed that eIF5 overexpression did not increase $(G_4C_2)_{80}$ repeat RNA levels in our cellular model (Fig. 1*G*). Moreover, even under eIF5-knockdown conditions, overexpression of siRNA-resistant eIF5 successfully rescued poly-GA expression (Fig. 1, *H* and *I*). This ruled out the possibility of off-target effects of eIF5 siRNAs. These results suggest that eIF5 stimulates poly-GA RAN translation in our cellular model of *C9orf72* repeat expansion.

eIF5 preferentially augments poly-GA translation over global translation

We then examined the extent to which eIF5 is selective for poly-GA RAN translation over global translation. To monitor the effect of eIF5 on global translation and estimate its selectivity on poly-GA RAN translation, we performed a puromycin incorporation assay on both eIF5 knockdown and eIF5 overexpression conditions (Fig. 2). To do knockdown, the cells were reverse transfected with eIF5 or nontargeting control siRNAs. Next day (day 1), cells were transfected with either $(G_4C_2)_{80}$ repeat plasmids or the corresponding mock plasmids. Twelve hours later, these cells were pulse labeled with puromycin, a structural analog of aminoacyl-tRNA. Puromycin is incorporated into the carboxy terminal of nascent polypeptides and labels neosynthesized proteins (56). As a negative control without pulse-labeling, puromycin-untreated cells were also prepared. Moreover, as a control for translation inhibition, a subset of cells was pretreated with cycloheximide (CHX), a translation elongation inhibitor, for 20 min (Fig. 2*A*). While whole cell lysates (input) of puromycin-labeled cells exhibited puromycin signals of various molecular weights (Fig. 2*B* lane 2–5), no puromycin signal was obtained from puromycin-untreated cells (Fig. 2*B* lane 1), and brief CHX treatment significantly decreased puromycin-labeled signals (Fig. 2*B* lane 5), thus supporting the successful monitoring of active cellular translation and the validity of our puromycin incorporation
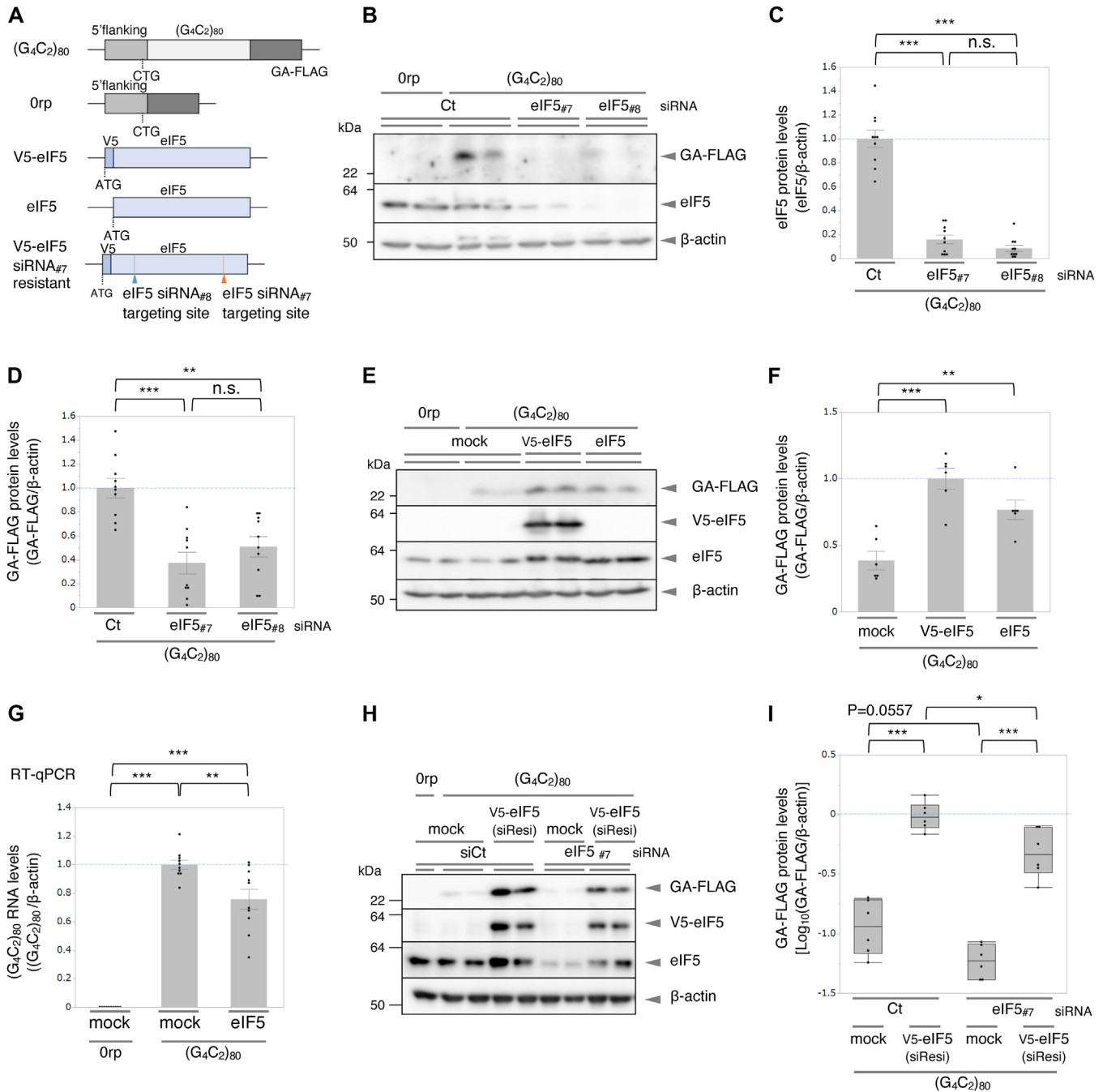
Figure 1. eIF5 stimulates poly-GA RAN translation. *A,* schematic representation of the plasmids used in the experiments is presented in this Figure. $(G_4C_2)_{80}$ repeat or control 0rp plasmid express 5′flanking region with or without $(G_4C_2)_{80}$. The repeat-containing transcript undergoes RAN translation, which produces poly-GA DPR C-terminally fused with a FLAG tag (GA-FLAG). N-terminally V5-tagged or untagged human eIF5 expression plasmid and an siRNA-resistant version (synonymous alteration of the siRNA for eIF5#7 targeting site) of the V5-tagged human eIF5 expression plasmid. A target site for siRNA eIF5#8 is also shown for reference. *B–D,* knockdown of eIF5 using two different target sequences (siRNAs #7, #8) decreased poly-GA expression in $(G_4C_2)_{80}$ repeat-expressing HeLa cells. Western blotting was performed with anti-FLAG, anti-eIF5, anti-β-actin antibodies. n = 5. Each experiment was performed in duplicates. *C* and *D,* ANOVA with Tukey-Kramer post hoc test. eIF5 and GA-FLAG protein levels in the graph were normalized by the signals of the control siRNA condition (Ct). *E* and *F,* coexpression of the V5-eIF5 or eIF5 plasmid increased poly-GA RAN translation in $(G_4C_2)_{80}$ repeat-expressing HeLa cells. Western blotting was performed with anti-FLAG, anti-V5, anti-eIF5, and anti-β-actin antibodies. n = 3. Experiments were performed in duplicates. ANOVA with Dunnett's post hoc test (*versus* mock). GA-FLAG protein levels in the graph were normalized by the signals of the $(G_4C_2)_{80}$ + V5-eIF5 transfection condition. *G,* RT-qPCR analysis quantifying G_4C_2 repeat RNA expression was normalized by β-actin mRNA. eIF5 expression suppresses cellular G_4C_2 repeat RNA expression. n = 4. Experiments were performed in duplicates. ANOVA with Tukey-Kramer post hoc test. G_4C_2 repeat RNA levels in the graph were normalized by the signals of $(G_4C_2)_{80}$ + mock transfection condition. *H* and *I,* eIF5 was knocked down using siRNA #7 and overexpressed using siRNA#7-resistant-V5-eIF5 in $(G_4C_2)_{80}$ repeat (siResi)-expressing HeLa cells. Western blotting was performed with anti-FLAG, anti-V5, anti-eIF5, and anti-β-actin antibodies. n = 3. Each experiment was performed in duplicates. ANOVA with Tukey-Kramer post hoc test. GA-FLAG protein levels in the graph were normalized by the signals of $(G_4C_2)_{80}$ + mock transfection under control siRNA condition and converted to ordinary logarithms. A *dot* in graphs represents a data point from single well of cell culture plate. (*C–I*) Graphs are presented as the mean ± standard error mean. (*C–I*) *p < 0.05, **p < 0.01, ***p < 0.001. DPR, dipeptide repeat proteins; eIF, eukaryotic translation initiation factor; GA, glycine-alanine; RAN, repeat associated non-AUG.
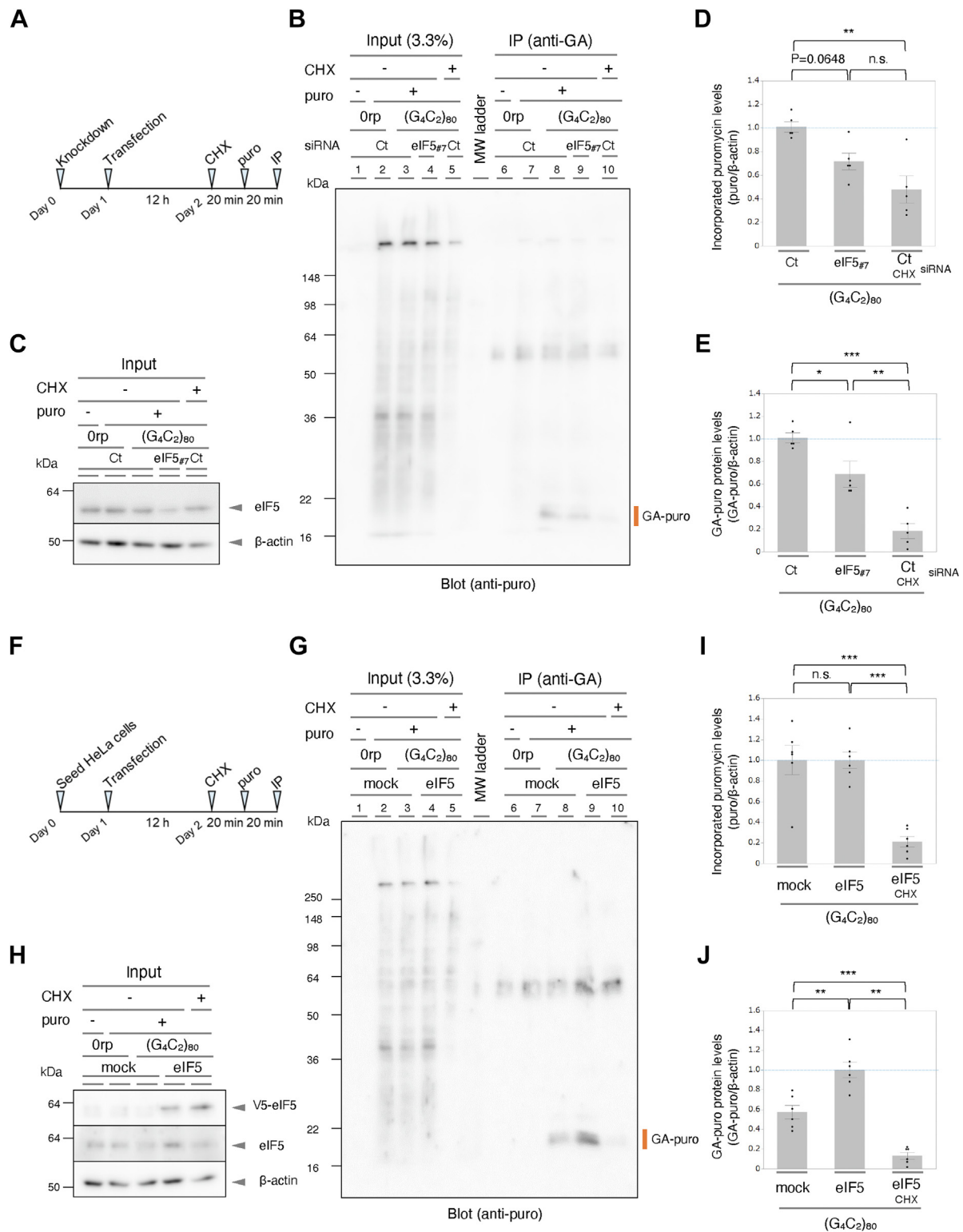
Figure 2. eIF5 preferentially stimulates poly-GA RAN translation over global translation. *A*, schematic representation of the experimental time-course of the modified puromycin incorporation assay with or without eIF5 knockdown. eIF5 or control siRNA were reverse transfected at cell seeding (day 0), The next day, $(G_4C_2)_{80}$ or mock plasmids were transfected (day 1). Twelve hours later, cells were treated with puromycin (puro) for 20 min to monitor global translation. A subset of cells was pretreated with the translation inhibitor cycloheximide (CHX) as a negative control for puromycin incorporation. Whole cell lysates were immunoprecipitated (IP) with anti-poly-GA antibodies. The whole cell lysates and immunoprecipitants were served for Western blotting. *B*, representative signals from anti-puromycin antibodies. n = 5. *C*, representative signals from anti-eIF5 and anti-β-actin antibodies, corresponding input lanes of Figure 2*B*. n = 5. *D*, quantification of incorporated puromycin signals from puromycin blots (*B*, whole lanes 3, 4, and 5) normalized by corresponding β-actin signals (*C*). n = 5. ANOVA with Tukey-Kramer post hoc test. The incorporated puromycin levels in the graph were normalized by the signals of "control knockdown + $(G_4C_2)_{80}$ transfection" condition. *E*, quantifications of signals of nascent poly-GA incorporating puromycin (GA-puro) from puromycin blots (*B*, lanes 8, 9, 10) were normalized by the corresponding β-actin signals (*C*). n = 5. ANOVA with Tukey-Kramer post hoc test. GA-puro protein levels in the graph were normalized by the signals of the "control knockdown+$(G_4C_2)_{80}$ transfection" condition. A *dot* in graphs represents a data point from single well of cell

assay. Knockdown of eIF5 (Fig. 2C) showed a tendency toward reduced puromycin incorporation, thus global nascent translation; however, this reduction did not reach statistical significance (Fig. 2B, lanes 3 and 4, Fig. 2D). Next, to examine the effect of eIF5 knockdown on the levels of puromycin-labeled nascent poly-GA, poly-GA in cell lysates (input) was concentrated by immunoprecipitation with an anti-GA antibody. The immunoprecipitates were then immunoblotted with an anti-puromycin antibody to examine the signals of puromycin-labeled nascent poly-GA (Fig. 2B lane 7–10). The nascent poly-GA signals (GA-puro) were detected only in the presence of $(G_4C_2)_{80}$ repeats (Fig. 2B lane 8–10) in the lower molecular weight range, compared to the detection of poly-GA using a FLAG tag located at the C terminus (Fig. 1H). This is assumed to be because the active translation of poly-GA was stopped midway owing to the incorporation of puromycin. Pretreatment with the elongation inhibitor CHX on control knockdown condition inhibited nascent poly-GA, further supporting the validity of our assay (Fig. 2B, lane 8 and 10, Fig. 2E). Importantly, eIF5 knockdown significantly reduced puromycin-labeled nascent poly-GA signals (Fig. 2B, lanes 8 and 9, Fig. 2E). These results suggest that knockdown of eIF5 selectively decreases poly-GA RAN translation compared with global translation.

Conversely, we next examined the selectivity of the effect of eIF5 overexpression on poly-GA RAN translation. To do so, cells were transfected with $(G_4C_2)_{80}$ repeat plasmids together with either eIF5 or the corresponding mock plasmids. These cells were then pulse labeled with puromycin (Fig. 2F). Overexpression of eIF5 (Fig. 2H) did not stimulate puromycin incorporation, thus, did not appear to stimulate global protein synthesis (Fig. 2G, lanes 3 and 4, Fig. 2I). Next, the expression levels of nascent poly-GA were examined through immunoprecipitation with an anti-GA antibody and immunoblotted with an anti-puromycin antibody. This revealed that eIF5 overexpression increased puromycin-labeled nascent poly-GA signals (Fig. 2G, lanes 8 and 9, Fig. 2J).

Collectively, these results suggest that eIF5 selectively increases poly-GA RAN translation compared to global translation.

eIF5 stimulates poly-GA translation through its intrinsic GAP activity and eIF2 binding

Next, we investigated the mechanism by which eIF5 stimulates poly-GA RAN translation. eIF5 is a GAP that accelerates the hydrolysis of GTP to GDP during translation initiation processes (45, 57). Therefore, we investigated whether GAP

activity is involved in eIF5-mediated augmentation of poly-GA RAN translation. GAP activity is critically dependent on the positive charge of arginine (R)15 of eIF5 in its N-terminal domain (45, 46), and the R15M substitution abolishes GAP activity, while eIF2-binding is not affected (46) (Fig. 3A). Coexpression of eIF5 R15M mutant with the $(G_4C_2)_{80}$ repeat showed a compromised augmentation of poly-GA RAN translation compared to that of the WT version of eIF5 (Fig. 3, B–D). There was no significant difference in the expression levels of WT eIF5 and its R15M mutant (Fig. 3C). These results suggest that eIF5 stimulation of poly-GA RAN translation requires its intrinsic GAP activity.

To gain a more mechanistic insight into the role of eIF5 in RAN translation stimulation, we analyzed whether the eIF5-eIF2 interaction was necessary for this activity. It is well established that eIF5-eIF2 binding is mediated through the eIF5 C-terminal domain (CTD) (58) and that the W391F mutation in the CTD of eIF5 diminishes the affinity of eIF5-eIF2 binding (58) (Fig. 3A). Therefore, we tested whether the W391F substitution in eIF5 attenuated the augmentation of poly-GA RAN translation. There was no significant difference in the expressions of eIF5 and its W391F mutant (Fig. 3C). Indeed, the W391F substitution impaired the stimulatory effect of poly-GA RAN translation from the $(G_4C_2)_{80}$ repeats (Fig. 3, B and D).

When combined, these results suggest that eIF5 stimulates poly-GA RAN translation through its intrinsic GAP activity and its binding to eIF2 through its CTD.

eIF5's effect on RAN translation does not require increased eIF2α phosphorylation

Although precise mechanism is unclear, it has been reported that RAN translation is stimulated during cellular integrated stress responses (ISR), which involves phosphorylation of eIF2α at Ser51 (p-eIF2α) (30–32). We therefore investigated whether the effect of eIF5 on poly-GA RAN translation is altered by the stimulation or inhibition of the ISR (Fig. 4A).

Sodium arsenite causes cellular oxidative stress and induces ISR, including induction of p-eIF2α, while ISRIB inhibits ISR by directly binding to eIF2B, increasing its guanine nucleotide exchange factor activity to increase GTP-bound eIF2, regardless of the phosphorylation state of eIF2α (59, 60). Sodium arsenite treatment of G_4C_2 repeat-expressing cells concurrently increased p-eIF2α level (Fig. 4, B and C) and the expression of poly-GA (Fig. 4, B and D). In contrast, treatment of G_4C_2 repeat-expressing cells with ISRIB did not reduce poly-GA expression from G_4C_2 repeats (Fig. 4, B and D),

---

culture plate. *F*, schematic representation of the experimental time-course of the modified puromycin incorporation assay for nascent poly-GA with or without eIF5 overexpression. One day after the cotransfection of the $(G_4C_2)_{80}$ and V5-eIF5 plasmids (day 2), the cells were pulse-labeled with puro, and subsequent procedures were carried out in the same way as above. *G*, representative signals from anti-puromycin antibodies. n = 6. *H*, representative signals from anti-V5, anti-eIF5 and anti-β-actin antibodies, corresponding input lanes of Figure 2*G*. n = 6. *I*, quantification of incorporated puromycin signals from puromycin blots (*G*, whole lanes 3, 4, and 5) normalized by corresponding β-actin signals (*H*). n = 6. ANOVA with Tukey-Kramer post hoc test. The incorporated puromycin levels in the graph were normalized by the signals of $(G_4C_2)_{80}$ + V5-eIF5 transfection condition. *J*, quantifications of signals of nascent poly-GA incorporating puromycin (GA-puro) from puromycin blots (*G*, lanes 8, 9, 10) were normalized by the corresponding β-actin signals (*H*). n = 6. ANOVA with Tukey-Kramer post hoc test. GA-puro protein levels in the graph were normalized by the signals of the $(G_4C_2)_{80}$ + eIF5 transfection condition. A *dot* in graphs represents a data point from single well of cell culture plate. (*D, E, I,* and *J*) Graphs are presented as the mean ± standard error mean.*$p < 0.05$, **$p < 0.01$, ***$p < 0.001$, n.s. indicates not significant. eIF, eukaryotic translation initiation factor; GA, glycine-alanine; RAN, repeat associated non-AUG.
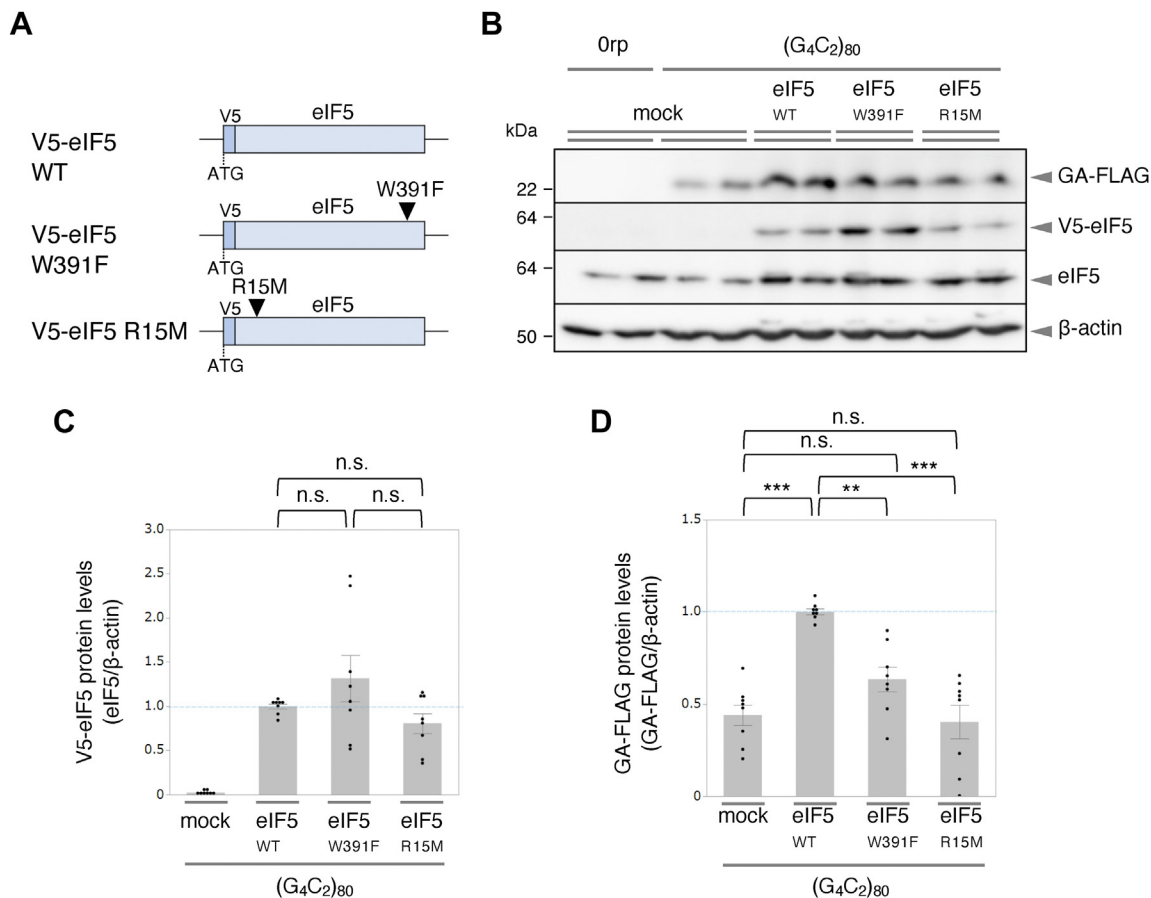
Figure 3. GAP activity and eIF2 binding are required for the eIF5-mediated stimulation of poly-GA RAN translation. *A*, schematic diagram of the N-terminal V5-tagged eIF5 (eIF5-WT) plasmid and its variants. *B–D*, V5-eIF5 W391F or V5-eIF5 R15M but not V5-eIF5 WT; the expression failed to increase poly-GA RAN translation from cotransfected $(G_4C_2)_{80}$ repeat. Western blotting signals from anti-FLAG, anti-V5, anti-eIF5, and anti-β-actin antibodies are shown. n = 4. Experiments were performed in duplicates. *C* and *D*, graphs are normalized by the signals of $(G_4C_2)_{80}$ + mock transfection and are presented as the mean ± standard error mean. ANOVA with Tukey-Kramer post hoc test. **$p < 0.01$, ***$p < 0.001$, n.s. indicates not significant. A *dot* in the graphs represents a data point from single well of cell culture plate. eIF, eukaryotic translation initiation factor; GA, glycine-alanine; GAP, GTPase-activating protein; RAN, repeat associated non-AUG.

indicating that the level of basal ISR level in our system is not very strong.

Next, we examined the effect of V5-eIF5 overexpression on p-eIF2α and poly-GA RAN translation under ISR induction or inhibition (Fig. 4B). p-eIF2α/eIF2α ratio showed no significant difference between with or without V5-eIF5 overexpression irrespective of ISR conditions (Fig. 4, *B, E, F,* and *G*); however, V5-eIF5 overexpression stimulated poly-GA RAN translation both in ISR induction or inhibition conditions (Fig. 4, *B, H, I,* and *J*). Collectively, the observed increase in poly-GA RAN translation by V5-eIF5 overexpression does not require increased eIF2α phosphorylation. Moreover, ISR induction by sodium arsenite and eIF5 overexpression have an additive effect on stimulating poly-GA RAN translation.

eIF5 acts primarily at the putative poly-GA initiation site

In global translation, eIF5 has been reported to increase non-AUG initiation, particularly CUG initiation (50, 61). Coinciding with these reports, poly-GA RAN translation in *C9orf72*-expanded G_4C_2 repeat is postulated to be initiated at CUG codon in the 5′ leader sequence (−24 bases) of G_4C_2

repeat (30, 53, 54). Therefore, we investigated whether eIF5 stimulates poly-GA RAN translation through the CUG codon. To test the possibility, we introduced CUG to C<u>C</u>G substitution in the 5′ leader sequence of the $(G_4C_2)_{80}$ repeat plasmid (CUG-$(G_4C_2)_{80}$) (Fig. 5A) and transfected to the cells. This revealed that the C<u>C</u>G substitution completely abolished the poly-GA signals, irrespective of the presence or absence of eIF5 overexpression (Fig. 5B). This result suggests that poly-GA RAN translation initiates at the CUG codon in our system, and the effect of eIF5 is dependent on the CUG initiation site and not on other potential alternative start sites.

To further characterize the CUG dependency of eIF5, next, we introduced CUG to <u>A</u>UG substitution in the 5′ leader sequence of the $(G_4C_2)_{80}$ repeat plasmid (<u>A</u>UG-$(G_4C_2)_{80}$) (Fig. 5A). As expected, the CUG to <u>A</u>UG substitution strongly stimulated poly-GA expression by efficiently initiating translation (Fig. 5, *C* and *D*). Intriguingly, eIF5 overexpression stimulated poly-GA RAN translation of the original CUG-$(G_4C_2)_{80}$ repeats but not that of the <u>A</u>UG-$(G_4C_2)_{80}$ repeats (Fig. 5, *C* and *D*). Thus, the CUG to <u>A</u>UG substitution abolished the eIF5-mediated stimulation of poly-GA RAN translation (Fig. 5, *C* and *D*). These results suggest that eIF5
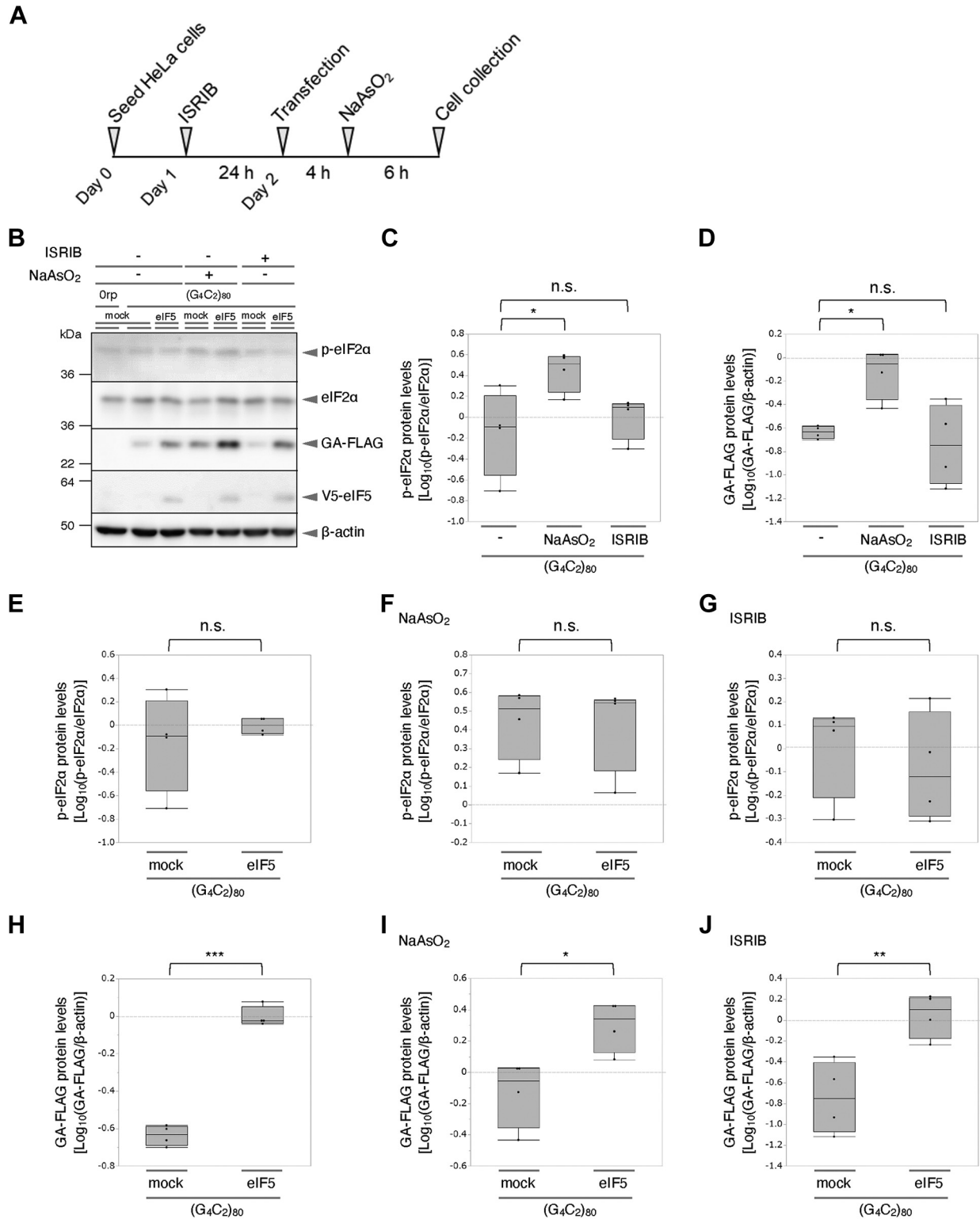
Figure 4. eIF5 and the integrated stress response additively stimulate poly-GA RAN translation, but eIF5 does not induce phosphorylation of eIF2α. *A*, schematic representation of the experimental time-course of the integrated stress response experiments. *B*, Western blotting signals from anti-p-eIF2α, anti-eIF2α, anti-FLAG, anti-V5, and anti-β-actin antibodies are shown. n = 4. *C*, quantification of p-eIF2α/eIF2α signals in ordinary logarithms normalized by the signal without NaAsO₂ or ISRIB treatment. n = 4. ANOVA with Tukey-Kramer post hoc test. *D*, quantification of GA-FLAG/β-actin signals in ordinary logarithms normalized by the signal without NaAsO₂ or ISRIB treatment. n = 4. ANOVA with Tukey-Kramer post hoc test. *E–G*, quantification of p-eIF2α/eIF2α signals in the presence or absence of eIF5 overexpression in control (*E*), NaAsO₂ treatment (*F*), or ISRIB treatment (*G*) conditions. n = 4. Unpaired two-tailed *t* test. *H–J*, quantification of GA-FLAG/β-actin signals in the presence or absence of eIF5 overexpression in control (*H*), NaAsO₂ treatment (*I*), or ISRIB treatment (*J*) conditions. n = 4. Unpaired two-tailed *t* test. Graphs are presented in ordinary logarithms in box-and-whisker plot (the central band is the median the ends of the box represent the first and third quartile, the whiskers extend from the ends of the box to the outermost data point that falls within "third quartile + 1.5 × interquartile range" to "first quartile - 1.5 × interquartile range"). (*C–J*) *$p < 0.05$, **$p < 0.01$, ***$p < 0.001$, n.s. indicates not significant. A *dot* in graphs represents a data point from single well of cell culture plate. eIF, eukaryotic translation initiation factor; GA, glycine-alanine; RAN, repeat associated non-AUG.
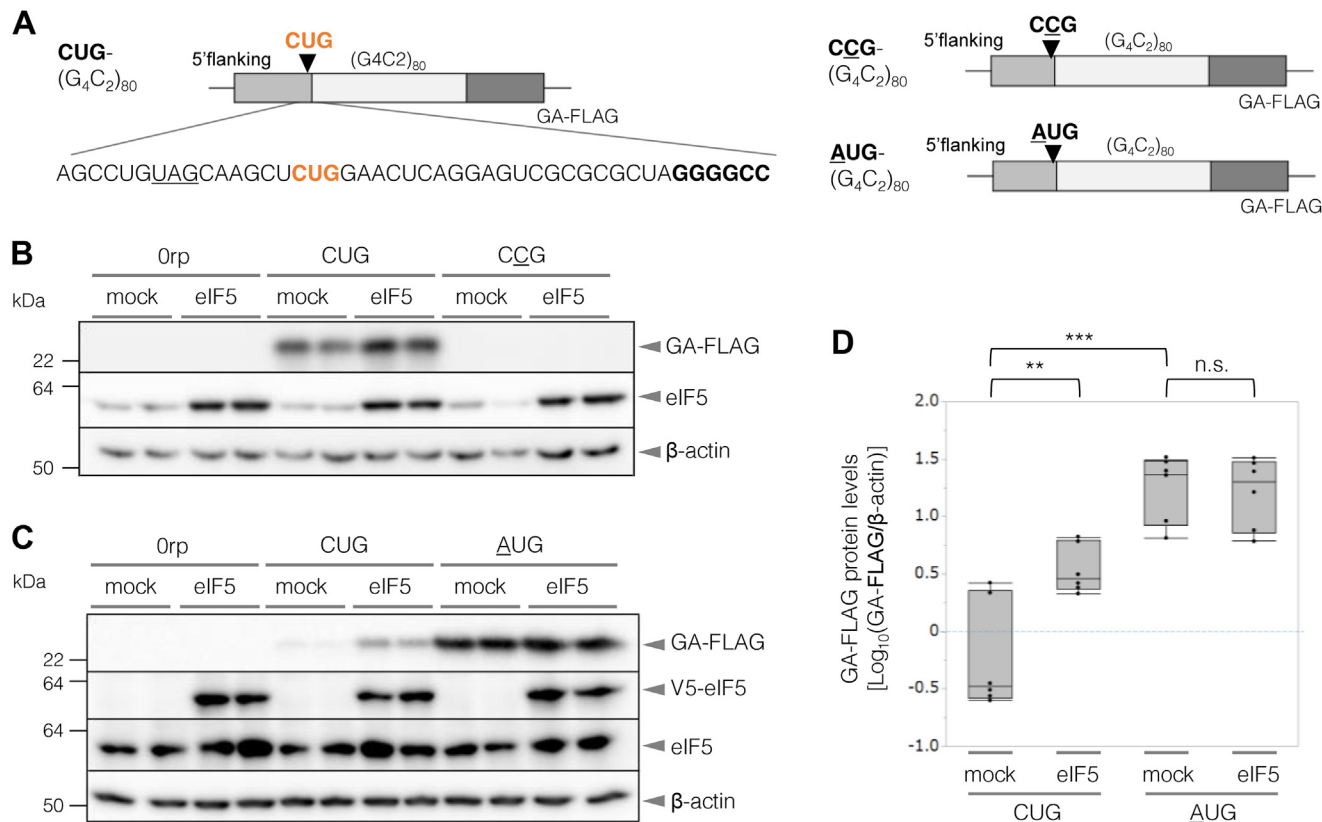
Figure 5. The disruption of the CUG initiation site abolishes the eIF5-mediated augmentation of poly-GA RAN translation. *A*, schematic representation of CUG-$(G_4C_2)_{80}$, C$\underline{C}$G-$(G_4C_2)_{80}$, and $\underline{A}$UG-$(G_4C_2)_{80}$ plasmids. Nucleotide sequence in 5′ leader sequences (repeat franking region) are shown. *B*, the CUG to C$\underline{C}$G substitution in 5′ leader sequence of $(G_4C_2)_{80}$ canceled poly-GA RAN translation in HeLa cells. Western blotting signals from anti-FLAG, anti-eIF5, and anti-β-actin antibodies are shown. n = 4. Experiments were performed in duplicates. *C* and *D*, V5-eIF5 failed to stimulate poly-GA translation in $\underline{A}$UG-$(G_4C_2)_{80}$ expressing HeLa cells. Western blotting signals from anti-FLAG, anti-V5, anti-eIF5, and anti-β-actin antibodies are shown. n = 3. Experiments were performed in duplicates. Graph is shown in box-and-whisker plot (the central band is the median the ends of the *box* represent the first and third quartile, the whiskers extend from the ends of the *box* to the outermost data point that falls within "third quartile + 1.5 × interquartile range" to "first quartile - 1.5 × interquartile range"). GA-FLAG protein levels in the graph were normalized by the signals of CUG-$(G_4C_2)_{80}$ + mock transfection and converted to ordinary logarithms. ANOVA with Tukey-Kramer post hoc test. **$p < 0.01$, ***$p < 0.001$, n.s. indicates not significant. A *dot* in the graph represents a data point from single well of cell culture plate. eIF, eukaryotic translation initiation factor; GA, glycine-alanine; RAN, repeat associated non-AUG.

preferentially stimulates poly-GA RAN translation through the CUG near cognate codon in the 5′ leader sequence (−24 bases) of G_4C_2 repeat.

Reduction of eIF5 suppresses poly-GA RAN translation in a Drosophila *model of* C9-*FTLD/ALS*

To evaluate *in vivo* effect of reducing eIF5 on poly-GA RAN translation, we next examined previously established *Drosophila* model of *C9*-FTLD/ALS that expresses 44 repeats of (G_4C_2) in fly eyes using the *GMR-Gal4* driver (38).

Knockdown of endogenous eIF5 by two independent RNAi strains (UAS-*eIF5 IR1* and UAS-*eIF5-IR2*) significantly reduced poly-GA expressions in the fly eyes compared to control knockdown (UAS-*lacZ IR*) (Fig. 6, *A* and *B*). Thus, consistent with the results of our cellular model, reduction of eIF5 suppresses poly-GA RAN translation in a *Drosophila* model of *C9*-FTLD/ALS. Collectively, our results suggest that eIF5 stimulates initiation at the CUG near cognate codon during *C9orf72* poly-GA RAN translation.

Discussion

Here, we revealed that eIF5 can modulate *C9orf72* G_4C_2 repeat RAN translation in our cellular and *Drosophila* models of *C9*-FTLD/ALS. eIF5 stimulates RAN translation in the poly-GA reading frame in a CUG codon-dependent manner. Mechanistically, GAP-inactivated (R15M) or eIF2-eIF5 interaction-deficient (W391F) eIF5 failed to enhance poly-GA RAN translation, suggesting that GAP activity and eIF2−eIF5 interactions are required for eIF5 to stimulate poly-GA RAN translation. Puromycin-incorporation assay revealed that eIF5 preferentially increased RAN translation over global translation. Moreover, disruption of near cognate codon (CUG to C$\underline{C}$G, CUG to $\underline{A}$UG) of poly-GA frame in the 5′ leader sequence of G_4C_2 repeat abolished the eIF5-mediated increase of poly-GA RAN translation. These results indicated that eIF5 preferentially stimulates the initiation of poly-GA RAN translation at the CUG codon. Additionally, the abolished effect of eIF5 on CUG to AUG initiation mutation may also be due to the relatively optimal sequence context of the mutated initiation site, as eIF5 has been reported to
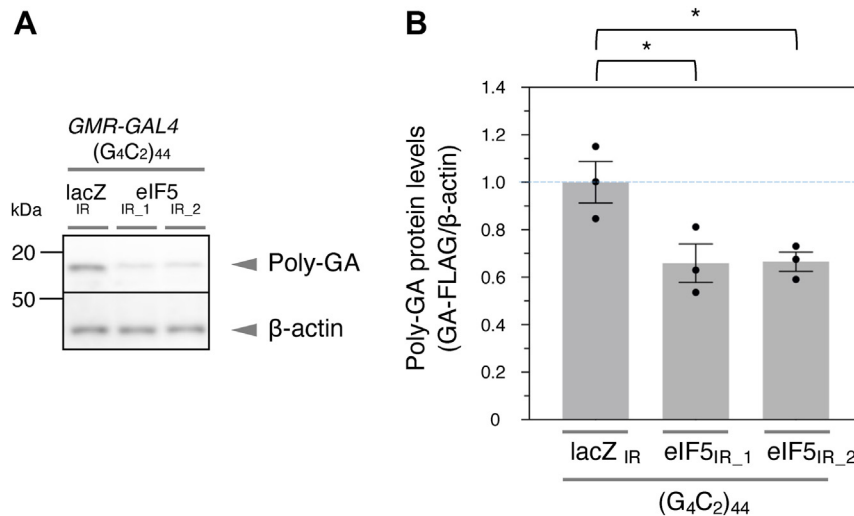
A

B

Figure 6. eIF5 stimulates poly-GA RAN translation in flies. *A* and *B*, heads of transgenic flies expressing the UAS-*LDS*-$(G_4C_2)_{44}$ and either UAS-*lacZ*$_{IR}$ (negative control), UAS-*eIF5*$_{IR\_1}$, or UAS-*eIF5*$_{IR\_2}$ transgenes under the control of the *GMR-Gal4* driver were served for Western blotting. Reduction of eIF5 decreased poly-GA expression in $(G_4C_2)_{44}$ repeat-expressing flies. Western blotting was performed with anti-poly-GA (Millipore #MABN889), anti-β-actin antibodies. n = 3. *$p < 0.05$; ANOVA with Dunnett's post hoc test (*versus* lacZ$_{IR}$). GA protein levels in the graph were normalized by the signals of the control condition (lacZ$_{IR}$). Graph is presented as the mean ± standard error mean. A *dot* in the graph represents a data point. eIF, eukaryotic translation initiation factor; GA, glycine-alanine; RAN, repeat associated non-AUG.

stimulate AUG initiation in the poorer Kozak consensus context (51).

Although eIF5 is a component of the 43S preinitiation complex identified more than 40 years ago (62), the extent to which it contributes to general translation is not fully clear relative to its long history (63, 64). eIF5 variants that impair eIF2 binding (W391F) or GAP activity (R15M) lose their stimulatory activity in poly-GA RAN translation, suggesting that eIF5 activity is mediated by the eIF2 complex. ISR-induced eIF2α phosphorylation at Ser51 leads to upregulation of RAN translation (30, 31). However, the precise mechanism of how cellular stress upregulates RAN translation remains largely unclear. In our study, overexpression of eIF5 did not increase the phospho-eIF2α/eIF2α ratio, while increasing poly-GA RAN translation. Moreover, neither the induction of ISR by sodium arsenite nor the reduction of ISR by ISRIB prevented eIF5-dependent stimulation of poly-GA RAN translation. While RAN translation is indeed stimulated under ISR condition (30–32), the effect of eIF5 on RAN translation may not be restricted to ISR condition at least in our system. These results together suggest that the stimulation of CUG-dependent initiation of poly-GA RAN translation by eIF5 may function independently or downstream of phosphorylation of eIF2α.

Although our data provide evidence that eIF5 stimulates RAN translation in a poly-GA reading frame in a CUG codon-dependent manner, further research is necessary, especially regarding the impact of eIF5 on RAN translation of other reading frames, such as poly-GP and poly-GR RAN translation. Although many studies agree on the initiation site of poly-GA RAN translation, the initiation sites of poly-GP and poly-GR in G_4C_2 strand remain controversial (52, 53, 65, 66). Some studies have claimed that frameshifts following CUG initiation are a source of poly-GP and poly-GR (52, 53). If this

is the case, the regulatory effect of eIF5 on CUG initiation may alter poly-GP and poly-GR expressions through a frameshift from the poly-GA reading frame during elongation. Alternatively, poly-GR is reported to be initiated by the AGG codon located (−1 to +2) in G_4C_2 repeats (29), although whether the AGG is indeed the initiation site of poly-GR remains controversial (66). If such non-CUG initiation occurs, eIF5 may also affect translation initiation efficacy as observed here in CUG-initiation, or there may be other factors that specifically affect translation initiation from each near cognate codon.

In this study, the stimulatory effect of eIF5 on poly-GA RAN translation over global translation was demonstrated in our cellular models, which was also supported in a *Drosophila* model of *C9orf72* FTLD/ALS, in which we observed poly-GA reduction on eIF5 knockdown. A limitation of the current study is that we could not monitor the effect of eIF5 knockdown on global translation in the *Drosophila* model. In addition, whether the effect of eIF5 on RAN translation is also seen in cells derived from carriers of *C9orf72* repeat expansions requires further study. Although the precise mechanism by which DPR drives neurodegeneration in patients remains unanswered, poly-GA accumulation has been linked to altered proteostasis (67) and neurodegeneration in various disease models (15, 17, 68, 69). Thus, the mechanism of stimulation of poly-GA RAN translation described here provides valuable insights into the precise mechanism of RAN translation regulation and a basis for the future development of selective RAN translation inhibitors as potential therapeutics for *C9*-FTLD/ALS. While we focused on G_4C_2 repeat expansion in *C9*-FTLD/ALS, it would also be intriguing to study whether eIF5 plays a regulatory role in RAN translation of other disease-related repeat expansions (70, 71).

Collectively, eIF5 preferentially stimulated the CUG initiation of poly-GA RAN translation from *C9orf72* G_4C_2 repeat.

eIF5 stimulates poly-GA RAN translation

Our data provide a mechanistic basis for regulating initiation codon selectivity in the RAN translation in *C9*-FTLD/ALS.

Experimental procedures

Cell culture

HeLa cells were cultured in Dulbecco's modified Eagle's medium containing 10% FCS and penicillin 100 U/ml/and streptomycin 100 μg/ml.

Fly stocks

All fly stocks were cultured and crossed at 25 °C in standard cornmeal-yeast-glucose medium. Transgenic flies bearing the *GMR-Gal4*, UAS-*lacZ IR*, and UAS-*LDS-(G₄C₂)₄₄* transgenes were described previously ([38](), [72](), [73]()). Transgenic flies bearing the UAS-*eIF5 IR1* and UAS-*eIF5-IR2* were obtained from the Bloomington *Drosophila* Stock Center (#34841) or Vienna *Drosophila* Resource Center (#105992) ([74]()), respectively.

Plasmids

The $(G_4C_2)_{80}$ repeat plasmids have been previously described ([5](), [28]()). These plasmids are driven by EF1 or CMV promoter expressing endogenous 113 nucleotides of 5′ leader sequence of G_4C_2 repeat followed by 80 repeats of G_4C_2 and corresponding peptide tags in each reading frame. The 5′ leader sequence contains CTG (−24 to −22 nucleotides from the first G of G_4C_2 repeat) near cognate codon that were proposed to be the initiation codons of poly-GA. CTG to C<u>C</u>G or <u>A</u>TG substitutions in the 5′ leader sequence were introduced through oligonucleotide ligation. To avoid autoregulation of eIF5 ([50]()), eIF5 coding sequence, but not its upstream open reading frame, was subcloned from plasmid human ORF clone pF1KB5142 (Kazusa DNA Res. Inst). The N-terminal V5 tag was fused to the eIF5 coding sequence by PCR and cloned into the HindIII/XhoI sites of the pcDNA5/FRT/TO vector (Invitrogen). siRNA-resistant version {synonymous alteration of the siRNA#7 targeting site GATGTA<u>T</u>GA<u>C</u>GC<u>C</u>GA<u>T</u>CT<u>G</u> [underlined where substitutions were introduced (GenScript)]} of the V5-tagged human eIF5 expression plasmid. The R15M and W391F point mutations of eIF5 were introduced by site-directed mutagenesis PCR.

Antibodies & reagent

The following antibodies were used at the indicated dilutions: anti-β-actin [(Sigma #A5316) 1/1000 or (Cell Signaling #47778) 1/2000] or (Sigma #A4700) 1/3000, anti-DYKDDDDK (FLAG) Tag (Cell Signaling #2368S) 1/1000, anti-eIF5 (D5G9) (Cell Signaling #13894) 1/2000, anti-V5 Tag (abcam #ab27671) 1/1000, anti-puromycin (MERCK #MABE343) 1/25,000, anti-poly-GA (Proteintech #24492-1-AP) 1/1000 or (Millipore #MABN889) 1/1000, anti-eIF2α (D7D3) (Cell signaling #5324) 1/1000, and anti-Phospho-eIF2α(Ser51) (Cell signaling #3398) 1/500. The following reagents were used: puromycin (nakarai tesque #14861-71), CHX (nakarai tesque #06741-91, CAS 66-81-9), Halt Protease and Phosphatase Single-Use Inhibitor Cocktail (100×) (Thermo #78442), ISRIB (Sigma #SML0843), Sodium Arsenite (Sigma #S7400), and Anti-Rabbit IgG (H + L), HRP conjugate (Promega #W401B), Anti-mouse IgG (H + L), and HRP conjugate (Promega #W402B).

siRNA-mediated knockdown and plasmid transfection

In knockdown experiments, HeLa cells cultured in 24-well plates, and 5 pmol of siRNA/well of 24-well plates were reverse-transfected with RNAiMAX reagent (Invitrogen) and incubated overnight. In the overexpression experiments, repeat plasmids and/or eIF5 plasmids were transfected using the lipofectamine LTX reagent (Invitrogen). Six hours after transfection, the medium was replaced with fresh medium. The following day, cells were washed with PBS and used for subsequent analyses. The siRNA sequences used for knockdown experiments were as follows: ON-TARGETplus Non-targeting siRNA #1 (Thermo): UGGUUUACAUGUCGACUAA; ON-TARGETplus Human EIF5 (1983) siRNA#7 (Thermo): GAUGUACGAUGCAGACCUU; ON-TARGETplus Human EIF5 (1983) siRNA#8 (Thermo): CAACGUAUCCCACCAAAUA.

Western blotting

Cells were dissolved in a RIPA buffer supplemented with a Protease Inhibitor Cocktail (Sigma) with EDTA and sonicated using a Bioruptor II. The samples were boiled for 10 min in the presence of 1 × SDS loading buffer. The samples were loaded onto a 10% to 12% Tris-glycine gel. After SDS-PAGE, samples were transferred onto PVDF membranes (Merck). After blocking with I-block (Thermo) for 1 h, the membrane was incubated overnight with a diluted primary antibody. The following day, the membrane was washed three times with TBST for 5 min and incubated with an HRP-labeled secondary antibody for 60 min. The cells were then washed thrice with TBST for 10 min. Chemiluminescent signals were detected using an Amersham Imager 600 or 680 (GE Healthcare). Signals were quantified using the Multi Gauge software (version 3.0; Fujifilm).

Western blotting of flies

Five heads of 3-day-old female adult flies were homogenized in 150 μl of sample buffer (125 mM Tris-HCl [pH 6.8], 20% glycerol, 4% SDS, 0.01% bromophenol blue dye, 10% 2-β-mercaptoethanol) with Biomasher II (Funakoshi). Homogenized heads were boiled for 5 min and then centrifuged at 10,000*g* for 3 min at 25 °C. Ten microliter of each supernatant was loaded on 5 to 20% gradient polyacrylamide gels (Atto) and then transferred onto Immun-Blot PVDF membranes (Bio-Rad). Membranes were blocked with PVDF blocking reagent for Can Get Signal (TOYOBO) at RT for 1 h and then incubated overnight at 4 °C with diluted primary antibodies. After washing three times with TBST, membranes were incubated at RT for 1 h with HRP-labeled secondary antibodies, then washed three times with TBST again. The chemiluminescent signals were visualized using ImmunoStar Zeta or ImmunoStar LD (Wako) and captured by Amersham Imager 600 (GE healthcare). Signals were quantified with ImageJ software (NIH).

RT-qPCR

HeLa cells cultured in 12-well plates were cotransfected with $(G_4C_2)_{80}$ repeat and eIF5 plasmids or corresponding mock plasmids. Total RNA was extracted using a RNeasy MINI Kit (QIAGEN) and a QIA shredder. Two micrograms RNA was reverse transcribed using Oligo dT(Invitrogen) and M-MLV (Promega). RT-qPCR was performed using the ViiA7 Real-Time PCR System (Applied Biosystems). Signals from repeat RNA were normalized by signals from β-actin according to the $\Delta\Delta C_T$ method. The primers used for RT-qPCR analysis were as follows:

Taq Man Primer targeting repeat TAG region (28).

Primer 1 TCTCAAACTGGGATGCGTAC, Primer 2 GTAGTCAAGCGTAGTCTGGG, Probe/56-FAM/TGCAGA-TAT/Zen/CCAGCACAGTGGCG/3IABkFQ/Taq Man Primer targeting β-actin, Primer 1 CCTTGCACATGCCGGAG, Primer 2 ACAGAGCCTCGCCTTTG, Probe/56-FAM/TCATCCATG/Zen/GTGAGCTGGCGG/3IABkFQ/.

Modified puromycin-incorporation assay

Puromycin-incorporation assay was performed as previously described (75) with modification. As for eIF5 overexpression experiments, 12 h after the cotransfection of $(G_4C_2)_{80}$ repeat with eIF5 plasmids or corresponding mock plasmids, HeLa cells were treated in the presence or absence of 20 μM of CHX for 20 min followed by a 20-min pulse labeling of the ongoing translation using 10 μg/ml puromycin. As for eIF5 knockdown experiments, cells were reverse transfected with siRNA targeting eIF5 or nontargeting control siRNA at seeding. These cells were transfected with $(G_4C_2)_{80}$ repeat or corresponding mock plasmid. Pulse-labeling with puromycin and subsequent procedures were carried out in the same way as above described. Cells were collected after the PBS wash. Cell lysates in RIPA buffer, Protein A-coupled Mag Sepharose beads (Cytiva), and anti-GA antibodies were mixed and incubated overnight at 4 °C with rotation. Immunoprecipitated samples and input cell lysates were used for Western blotting. Puromycin-labeled proteins were immunoblotted using an anti-puromycin antibody. Anti-puromycin antibody signals were quantified and normalized to β-actin signals.

Induction or inhibition of integrated stress response in cultured cells

HeLa cells were seeded on 24-well culture plate (Day 0). Next day (Day 1), cells in indicated wells were treated with 2 μM ISRIB for 24 h. Then, culture medium was replaced with fresh (media for ISRIB-treated cell contains freshly prepared 2 μM ISRIB), and $(G_4C_2)_{80}$ repeat plasmids with or without eIF5 plasmids were transfected using the lipofectamine LTX reagent. After 4 h, the medium containing sodium arsenite was added to a final concentration of 200 μM. After 6 h of culture, cells were served for Western blotting.

Statistics

Statistical analysis was performed using JMP Pro 17 software and GraphPad Prism version 10.0.3.

Data availability

No large-scale datasets are associated with this study.

References

1. DeJesus-Hernandez, M., Mackenzie, I. R., Boeve, B. F., Boxer, A. L., Baker, M., Rutherford, N. J., *et al.* (2011) Expanded GGGGCC hexanucleotide repeat in noncoding region of C9ORF72 causes chromosome 9p-linked FTD and ALS. *Neuron* **72**, 245–256
2. Gijselinck, I., Van Langenhove, T., van der Zee, J., Sleegers, K., Philtjens, S., Kleinberger, G., *et al.* (2012) A C9orf72 promoter repeat expansion in a Flanders-Belgian cohort with disorders of the frontotemporal lobar degeneration-amyotrophic lateral sclerosis spectrum: a gene identification study. *Lancet Neurol.* **11**, 54–65
3. Renton, A. E., Majounie, E., Waite, A., Simon-Sanchez, J., Rollinson, S., Gibbs, J. R., *et al.* (2011) A hexanucleotide repeat expansion in C9ORF72 is the cause of chromosome 9p21-linked ALS-FTD. *Neuron* **72**, 257–268
4. Ash, P. E., Bieniek, K. F., Gendron, T. F., Caulfield, T., Lin, W. L., Dejesus-Hernandez, M., *et al.* (2013) Unconventional translation of C9ORF72 GGGGCC expansion generates insoluble polypeptides specific to c9FTD/ALS. *Neuron* **77**, 639–646
5. Mori, K., Weng, S. M., Arzberger, T., May, S., Rentzsch, K., Kremmer, E., *et al.* (2013) The C9orf72 GGGGCC repeat is translated into aggregating dipeptide-repeat proteins in FTLD/ALS. *Science* **339**, 1335–1338

6. Gendron, T. F., Bieniek, K. F., Zhang, Y. J., Jansen-West, K., Ash, P. E., Caulfield, T., *et al.* (2013) Antisense transcripts of the expanded C9ORF72 hexanucleotide repeat form nuclear RNA foci and undergo repeat-associated non-ATG translation in c9FTD/ALS. *Acta Neuropathol.* **126**, 829–844

7. Zu, T., Liu, Y., Banez-Coronel, M., Reid, T., Pletnikova, O., Lewis, J., *et al.* (2013) RAN proteins and RNA foci from antisense transcripts in C9ORF72 ALS and frontotemporal dementia. *Proc. Natl. Acad. Sci. U. S. A.* **110**, E4968–E4977

8. Mori, K., Arzberger, T., Grasser, F. A., Gijselinck, I., May, S., Rentzsch, K., *et al.* (2013) Bidirectional transcripts of the expanded C9orf72 hexanucleotide repeat are translated into aggregating dipeptide repeat proteins. *Acta Neuropathol.* **126**, 881–893

9. Mori, K., Gotoh, S., and Ikeda, M. (2023) Aspects of degradation and translation of the expanded C9orf72 hexanucleotide repeat RNA. *J. Neurochem.* **166**, 156–171

10. Jovicic, A., Mertens, J., Boeynaems, S., Bogaert, E., Chai, N., Yamada, S. B., *et al.* (2015) Modifiers of C9orf72 dipeptide repeat toxicity connect nucleocytoplasmic transport defects to FTD/ALS. *Nat. Neurosci.* **18**, 1226–1229

11. Tran, H., Almeida, S., Moore, J., Gendron, T. F., Chalasani, U., Lu, Y., *et al.* (2015) Differential toxicity of nuclear RNA foci *versus* dipeptide repeat proteins in a Drosophila model of C9ORF72 FTD/ALS. *Neuron* **87**, 1207–1214

12. Mizielinska, S., Gronke, S., Niccoli, T., Ridler, C. E., Clayton, E. L., Devoy, A., *et al.* (2014) C9orf72 repeat expansions cause neurodegeneration in Drosophila through arginine-rich proteins. *Science* **345**, 1192–1194

13. Kwon, I., Xiang, S., Kato, M., Wu, L., Theodoropoulos, P., Wang, T., *et al.* (2014) Poly-dipeptides encoded by the C9orf72 repeats bind nucleoli, impede RNA biogenesis, and kill cells. *Science* **345**, 1139–1145

14. Lee, K. H., Zhang, P., Kim, H. J., Mitrea, D. M., Sarkar, M., Freibaum, B. D., *et al.* (2016) C9orf72 dipeptide repeats impair the assembly, dynamics, and function of membrane-less organelles. *Cell* **167**, 774–788.e17

15. May, S., Hornburg, D., Schludi, M. H., Arzberger, T., Rentzsch, K., Schwenk, B. M., *et al.* (2014) C9orf72 FTLD/ALS-associated Gly-Ala dipeptide repeat proteins cause neuronal toxicity and Unc119 sequestration. *Acta Neuropathol.* **128**, 485–503

16. Cook, C. N., Wu, Y., Odeh, H. M., Gendron, T. F., Jansen-West, K., Del Rosso, G., *et al.* (2020) C9orf72 poly(GR) aggregation induces TDP-43 proteinopathy. *Sci. Transl. Med.* **12**, eabb3774

17. LaClair, K. D., Zhou, Q., Michaelsen, M., Wefers, B., Brill, M. S., Janjic, A., *et al.* (2020) Congenic expression of poly-GA but not poly-PR in mice triggers selective neuron loss and interferon responses found in C9orf72 ALS. *Acta Neuropathol.* **140**, 121–142

18. Mackenzie, I. R., Arzberger, T., Kremmer, E., Troost, D., Lorenzl, S., Mori, K., *et al.* (2013) Dipeptide repeat protein pathology in C9ORF72 mutation cases: clinico-pathological correlations. *Acta Neuropathol.* **126**, 859–879

19. Mackenzie, I. R., Frick, P., Grasser, F. A., Gendron, T. F., Petrucelli, L., Cashman, N. R., *et al.* (2015) Quantitative analysis and clinico-pathological correlations of different dipeptide repeat protein pathologies in C9ORF72 mutation carriers. *Acta Neuropathol.* **130**, 845–861

20. Schludi, M. H., May, S., Grasser, F. A., Rentzsch, K., Kremmer, E., Kupper, C., *et al.* (2015) Distribution of dipeptide repeat proteins in cellular models and C9orf72 mutation cases suggests link to transcriptional silencing. *Acta Neuropathol.* **130**, 537–555

21. Saberi, S., Stauffer, J. E., Jiang, J., Garcia, S. D., Taylor, A. E., Schulte, D., *et al.* (2018) Sense-encoded poly-GR dipeptide repeat proteins correlate to neurodegeneration and uniquely co-localize with TDP-43 in dendrites of repeat-expanded C9orf72 amyotrophic lateral sclerosis. *Acta Neuropathol.* **135**, 459–474

22. Gittings, L. M., Boeynaems, S., Lightwood, D., Clargo, A., Topia, S., Nakayama, L., *et al.* (2020) Symmetric dimethylation of poly-GR correlates with disease duration in C9orf72 FTLD and ALS and reduces poly-GR phase separation and toxicity. *Acta Neuropathol.* **139**, 407–410

23. Sakae, N., Bieniek, K. F., Zhang, Y. J., Ross, K., Gendron, T. F., Murray, M. E., *et al.* (2018) Poly-GR dipeptide repeat polymers correlate with neurodegeneration and clinicopathological subtypes in C9ORF72-related brain disease. *Acta Neuropathol. Commun.* **6**, 63

24. Shi, Y., Lin, S., Staats, K. A., Li, Y., Chang, W. H., Hung, S. T., *et al.* (2018) Haploinsufficiency leads to neurodegeneration in C9ORF72 ALS/FTD human induced motor neurons. *Nat. Med.* **24**, 313–325

25. Zhu, Q., Jiang, J., Gendron, T. F., McAlonis-Downes, M., Jiang, L., Taylor, A., *et al.* (2020) Reduced C9ORF72 function exacerbates gain of toxicity from ALS/FTD-causing repeat expansion in C9orf72. *Nat. Neurosci.* **23**, 615–624

26. Lee, Y. B., Chen, H. J., Peres, J. N., Gomez-Deza, J., Attig, J., Stalekar, M., *et al.* (2013) Hexanucleotide repeats in ALS/FTD form length-dependent RNA foci, sequester RNA binding proteins, and are neurotoxic. *Cell Rep.* **5**, 1178–1186

27. Cooper-Knock, J., Higginbottom, A., Stopford, M. J., Highley, J. R., Ince, P. G., Wharton, S. B., *et al.* (2015) Antisense RNA foci in the motor neurons of C9ORF72-ALS patients are associated with TDP-43 proteinopathy. *Acta Neuropathol.* **130**, 63–75

28. Mori, K., Nihei, Y., Arzberger, T., Zhou, Q., Mackenzie, I. R., Hermann, A., *et al.* (2016) Reduced hnRNPA3 increases C9orf72 repeat RNA levels and dipeptide-repeat protein deposition. *EMBO Rep.* **17**, 1314–1325

29. Boivin, M., Pfister, V., Gaucherot, A., Ruffenach, F., Negroni, L., Sellier, C., *et al.* (2020) Reduced autophagy upon C9ORF72 loss synergizes with dipeptide repeat protein toxicity in G4C2 repeat expansion disorders. *Embo J.* **39**, e100574

30. Green, K. M., Glineburg, M. R., Kearse, M. G., Flores, B. N., Linsalata, A. E., Fedak, S. J., *et al.* (2017) RAN translation at C9orf72-associated repeat expansions is selectively enhanced by the integrated stress response. *Nat. Commun.* **8**, 2005

31. Cheng, W., Wang, S., Mestre, A. A., Fu, C., Makarem, A., Xian, F., *et al.* (2018) C9ORF72 GGGGCC repeat-associated non-AUG translation is upregulated by stress through eIF2alpha phosphorylation. *Nat. Commun.* **9**, 51

32. Westergard, T., McAvoy, K., Russell, K., Wen, X., Pang, Y., Morris, B., *et al.* (2019) Repeat-associated non-AUG translation in C9orf72-ALS/FTD is driven by neuronal excitation and stress. *EMBO Mol. Med.* **11**, e9423

33. Zu, T., Guo, S., Bardhi, O., Ryskamp, D. A., Li, J., Khoramian Tusi, S., *et al.* (2020) Metformin inhibits RAN translation through PKR pathway and mitigates disease in C9orf72 ALS/FTD mice. *Proc. Natl. Acad. Sci. U. S. A.* **117**, 18591–18599

34. Yamada, S. B., Gendron, T. F., Niccoli, T., Genuth, N. R., Grosely, R., Shi, Y., *et al.* (2019) RPS25 is required for efficient RAN translation of C9orf72 and other neurodegenerative disease-associated nucleotide repeats. *Nat. Neurosci.* **22**, 1383–1388

35. Liu, H., Lu, Y. N., Paul, T., Periz, G., Banco, M. T., Ferre-D'Amare, A. R., *et al.* (2021) A helicase unwinds hexanucleotide repeat RNA G-quadruplexes and facilitates repeat-associated non-AUG translation. *J. Am. Chem. Soc.* **143**, 7368–7379

36. Cheng, W., Wang, S., Zhang, Z., Morgens, D. W., Hayes, L. R., Lee, S., *et al.* (2019) CRISPR-Cas9 screens identify the RNA helicase DDX3X as a repressor of C9ORF72 (GGGGCC)n repeat-associated non-AUG translation. *Neuron* **104**, 885–898.e8

37. Fujino, Y., Ueyama, M., Ishiguro, T., Ozawa, D., Ito, H., Sugiki, T., *et al.* (2023) FUS regulates RAN translation through modulating the G-quadruplex structure of GGGGCC repeat RNA in C9orf72-linked ALS/FTD. *Elife* **12**, RP84338

38. Goodman, L. D., Prudencio, M., Srinivasan, A. R., Rifai, O. M., Lee, V. M., Petrucelli, L., *et al.* (2019) eIF4B and eIF4H mediate GR production from expanded G4C2 in a Drosophila model for C9orf-associated ALS. *Acta Neuropathol. Commun.* **7**, 62

39. Sonobe, Y., Aburas, J., Krishnan, G., Fleming, A. C., Ghadge, G., Islam, P., *et al.* (2021) A C. elegans model of C9orf72-associated ALS/FTD uncovers a conserved role for eIF2D in RAN translation. *Nat. Commun.* **12**, 6025

40. Green, K. M., Miller, S. L., Malik, I., and Todd, P. K. (2022) Non-canonical initiation factors modulate repeat-associated non-AUG translation. *Hum. Mol. Genet.* **31**, 2521–2534

41. Si, K., Das, K., and Maitra, U. (1996) Characterization of multiple mRNAs that encode mammalian translation initiation factor 5 (eIF-5). *J. Biol. Chem.* **271**, 16934–16938

42. Raychaudhuri, P., Chaudhuri, A., and Maitra, U. (1985) Eukaryotic initiation factor 5 from calf liver is a single polypeptide chain protein of Mr = 62,000. *J. Biol. Chem.* **260**, 2132–2139

43. Raychaudhuri, P., Chaudhuri, A., and Maitra, U. (1985) Formation and release of eukaryotic initiation factor 2X GDP complex during eukaryotic ribosomal polypeptide chain initiation complex formation. *J. Biol. Chem.* **260**, 2140–2145

44. Algire, M. A., Maag, D., and Lorsch, J. R. (2005) Pi release from eIF2, not GTP hydrolysis, is the step controlled by start-site selection during eukaryotic translation initiation. *Mol. Cell* **20**, 251–262

45. Das, S., Ghosh, R., and Maitra, U. (2001) Eukaryotic translation initiation factor 5 functions as a GTPase-activating protein. *J. Biol. Chem.* **276**, 6720–6726

46. Paulin, F. E., Campbell, L. E., O'Brien, K., Loughlin, J., and Proud, C. G. (2001) Eukaryotic translation initiation factor 5 (eIF5) acts as a classical GTPase-activator protein. *Curr. Biol.* **11**, 55–59

47. Kozak, M. (1986) Point mutations define a sequence flanking the aug initiator codon that modulates translation by eukaryotic ribosomes. *Cell* **44**, 283–292

48. Hinnebusch, A. G. (2014) The scanning mechanism of eukaryotic translation initiation. *Annu. Rev. Biochem.* **83**, 779–812

49. Das, S., and Maitra, U. (2001) Functional significance and mechanism of eIF5-promoted GTP hydrolysis in eukaryotic translation initiation. *Prog. Nucleic Acid Res. Mol. Biol.* **70**, 207–231

50. Loughran, G., Sachs, M. S., Atkins, J. F., and Ivanov, I. P. (2012) Stringency of start codon selection modulates autoregulation of translation initiation factor eIF5. *Nucleic Acids Res.* **40**, 2898–2906

51. Pisareva, V. P., and Pisarev, A. V. (2014) eIF5 and eIF5B together stimulate 48S initiation complex formation during ribosomal scanning. *Nucleic Acids Res.* **42**, 12052–12069

52. Latallo, M. J., Wang, S., Dong, D., Nelson, B., Livingston, N. M., Wu, R., *et al.* (2023) Single-molecule imaging reveals distinct elongation and frameshifting dynamics between frames of expanded RNA repeats in C9ORF72-ALS/FTD. *Nat. Commun.* **14**, 5581

53. Tabet, R., Schaeffer, L., Freyermuth, F., Jambeau, M., Workman, M., Lee, C. Z., *et al.* (2018) CUG initiation and frameshifting enable production of dipeptide repeat proteins from ALS/FTD C9ORF72 transcripts. *Nat. Commun.* **9**, 152

54. Sonobe, Y., Ghadge, G., Masaki, K., Sendoel, A., Fuchs, E., and Roos, R. P. (2018) Translation of dipeptide repeat proteins from the C9ORF72 expanded repeat is associated with cellular stress. *Neurobiol. Dis.* **116**, 155–165

55. Kawabe, Y., Mori, K., Yamashita, T., Gotoh, S., and Ikeda, M. (2020) The RNA exosome complex degrades expanded hexanucleotide repeat RNA in C9orf72 FTLD/ALS. *EMBO J.* **39**, e102700

56. Schmidt, E. K., Clavarino, G., Ceppi, M., and Pierre, P. (2009) SUnSET, a nonradioactive method to monitor protein synthesis. *Nat. Methods* **6**, 275–277

57. Das, S., Maiti, T., Das, K., and Maitra, U. (1997) Specific interaction of eukaryotic translation initiation factor 5 (eIF5) with the beta-subunit of eIF2. *J. Biol. Chem.* **272**, 31712–31718

58. Jennings, M. D., and Pavitt, G. D. (2010) eIF5 has GDI activity necessary for translational control by eIF2 phosphorylation. *Nature* **465**, 378–381

59. Sidrauski, C., Acosta-Alvear, D., Khoutorsky, A., Vedantham, P., Hearn, B. R., Li, H., *et al.* (2013) Pharmacological brake-release of mRNA translation enhances cognitive memory. *Elife* **2**, e00498

60. Sekine, Y., Zyryanova, A., Crespillo-Casado, A., Fischer, P. M., Harding, H. P., and Ron, D. (2015) Stress responses. Mutations in a translation initiation factor identify the target of a memory-enhancing compound. *Science* **348**, 1027–1030

61. Nanda, J. S., Saini, A. K., Munoz, A. M., Hinnebusch, A. G., and Lorsch, J. R. (2013) Coordinated movements of eukaryotic translation initiation factors eIF1, eIF1A, and eIF5 trigger phosphate release from eIF2 in response to start codon recognition by the ribosomal preinitiation complex. *J. Biol. Chem.* **288**, 5316–5329

62. Benne, R., Brown-Luedi, M. L., and Hershey, J. W. (1978) Purification and characterization of protein synthesis initiation factors eIF-1, eIF-4C, eIF-4D, and eIF-5 from rabbit reticulocytes. *J. Biol. Chem.* **253**, 3070–3077

63. Kozak, M. (1999) Initiation of translation in prokaryotes and eukaryotes. *Gene* **234**, 187–208

64. Friedrich, D., Marintchev, A., and Arthanari, H. (2022) The metaphorical swiss army knife: the multitude and diverse roles of HEAT domains in eukaryotic translation initiation. *Nucleic Acids Res.* **50**, 5424–5442

65. Almeida, S., Krishnan, G., Rushe, M., Gu, Y., Kankel, M. W., and Gao, F. B. (2019) Production of poly(GA) in C9ORF72 patient motor neurons derived from induced pluripotent stem cells. *Acta Neuropathol.* **138**, 1099–1101

66. Lampasona, A., Almeida, S., and Gao, F. B. (2021) Translation of the poly(GR) frame in C9ORF72-ALS/FTD is regulated by *cis*-elements involved in alternative splicing. *Neurobiol. Aging* **105**, 327–332

67. Guo, Q., Lehmer, C., Martinez-Sanchez, A., Rudack, T., Beck, F., Hartmann, H., *et al.* (2018) *In Situ* structure of neuronal C9orf72 poly-GA aggregates reveals proteasome recruitment. *Cell* **172**, 696–705.e12

68. Lee, Y. B., Baskaran, P., Gomez-Deza, J., Chen, H. J., Nishimura, A. L., Smith, B. N., *et al.* (2017) C9orf72 poly GA RAN-translated protein plays a key role in amyotrophic lateral sclerosis *via* aggregation and toxicity. *Hum. Mol. Genet.* **26**, 4765–4777

69. Zhang, Y. J., Gendron, T. F., Grima, J. C., Sasaguri, H., Jansen-West, K., Xu, Y. F., *et al.* (2016) C9ORF72 poly(GA) aggregates sequester and impair HR23 and nucleocytoplasmic transport proteins. *Nat. Neurosci.* **19**, 668–677

70. Fujino, Y., Mori, K., and Nagai, Y. (2023) Repeat-associated non-AUG translation in neuromuscular diseases: mechanisms and therapeutic insights. *J. Biochem.* **173**, 273–281

71. Linsalata, A. E., He, F., Malik, A. M., Glineburg, M. R., Green, K. M., Natla, S., *et al.* (2019) DDX3X and specific initiation factors modulate FMR1 repeat-associated non-AUG-initiated translation. *EMBO Rep.* **20**, e47498

72. Yamaguchi, M., Hirose, F., Inoue, Y. H., Shiraki, M., Hayashi, Y., Nishi, Y., *et al.* (1999) Ectopic expression of human p53 inhibits entry into S phase and induces apoptosis in the Drosophila eye imaginal disc. *Oncogene* **18**, 6767–6775

73. Kennerdell, J. R., and Carthew, R. W. (2000) Heritable gene silencing in Drosophila using double-stranded RNA. *Nat. Biotechnol.* **18**, 896–898

74. Dietzl, G., Chen, D., Schnorrer, F., Su, K. C., Barinova, Y., Fellner, M., *et al.* (2007) A genome-wide transgenic RNAi library for conditional gene inactivation in Drosophila. *Nature* **448**, 151–156

75. Mori, K., Gotoh, S., Yamashita, T., Uozumi, R., Kawabe, Y., Tagami, S., *et al.* (2021) The porphyrin TMPyP4 inhibits elongation during the noncanonical translation of the FTLD/ALS-associated GGGGCC repeat in the C9orf72 gene. *J. Biol. Chem.* **297**, 101120